Lattice Cluster Theory for Pedestrians: The Incompressible Limit and the Miscibility of Polyolefin Blends

Karl F. Freed* and Jacek Dudowicz

James Franck Institute and Department of Chemistry, University of Chicago, Chicago, Illinois 60637

Received May 4, 1998; Revised Manuscript Received July 17, 1998

ABSTRACT: The high pressure (incompressible), high molecular weight limit of the lattice cluster theory is derived as a first approximation to describe the influence of monomer molecular structure and nonrandom mixing effects on the thermodynamic properties of binary polymer blends. In particular, the noncombinatorial free energy of mixing and the small angle neutron scattering effective interaction parameter χ_{exp} emerge in this limit as rather simple, compact analytical expressions that depend on a single microscopic energy and on two geometrical indices obtained easily from the monomer united atom structures. These analytical expressions, in conjunction with the geometrical indices summarized in a table for a wide range of vinyl monomer structures, enable the rapid use of the theory with minor additional effort than the application of Flory−Huggins theory. Our theory is applied to a few polyolefin blends in order (a) to illustrate a new mechanism for the occurrence of lower critical solution temperature (LCST) phase diagrams in incompressible systems, (b) to provide a partial explanation of why blends of poly(isobutylene) with other polyolefins often yields LCST behavior, and (c) to explain the rather large *negative* entropic portions of χ_{exp} observed for many binary polyolefin blends.

I. Introduction

Knowledge of the phase behavior of multicomponent polymer systems is an important ingredient in designing new materials with desired properties. The phase behavior of these systems is most often described by Flory−Huggins (FH) theory with the phenomenological Flory interaction parameter χ extracted from a variety of different experiments. This classic FH approach is quite successful in correlating data from different measurements and also is very helpful in understanding certain aspects of miscibility in polymer blends. For example, FH theory explains why most homopolymer blends are immiscible. Despite these important successes, FH theory displays several deficiencies which limit the theory from being a vehicle for predicting the properties of new multicomponent polymeric materials. A list of these deficiencies delineates the requirements that must be met by new, ambitious theories with greater predictive abilities.

The Flory parameter χ, as *derived* from FH theory,[1] is proportional to $1/T$, where T is the absolute temperature, and χ is independent of composition, molecular weights, and pressure. In contrast, experiments often indicate a dependence of χ on both composition and molecular weights, and, more recently, also on pressure.[2] Another serious departure of FH theory from observations concerns the temperature dependence of χ, which is generally found to be of the form $\chi = A + B/T$, where A is often called "the entropic χ". FH theory, on the other hand, yields the parameter A as identically zero. Moreover, FH theory is incapable of distinguishing between different polymer architectures (linear, comb, and star, polymers etc.) and between different types of copolymers (block, random, alternating) with the same compositions. These deficiencies are all quite serious and impede the predictive abilities of FH theory. For example, the experimental χ parameters, analyzed with FH theory, cannot provide meaningful microscopic molecular information that may be useful for designing materials with specified properties.

The lattice cluster theory[3−5] (LCT) has been formulated to alleviate the above deficiencies of FH theory. By combining a significantly more advanced solution to the lattice model of polymer systems[5,6] with a description of monomer molecular structures, the LCT has (a) explained the presence of the "entropic χ" as arising from the packing of monomers with different sizes and shapes,[7] (b) demonstrated the general occurrence of a composition and molecular weight dependence[8] of χ as a consequence of the combined influences of monomer molecular structure, compressibility, and nonrandom mixing effects, (c) predicted the pressure dependence[9] of χ (subsequently verified experimentally), (d) described the dependence of χ on chain architecture and on the monomer sequence in copolymers,[10] and (e) provided predictions of novel phenomena, such as the ordering of certain block copolymers upon heating.[11,12] Most recently, LCT computations have explained[13] the molecular origins of the observed[14] significantly different miscibilities of poly(ethylene propylene) with atactic and head-to-head poly(propylene).

Greater complexity emerges as an inevitable consequence of *any* theory that can yield these significant advances. Thus, the more lengthy expressions for the LCT free energy appear because the theory explicitly describes monomer molecular structures,[4,5] nonrandom mixing, and blend compressibility. The inclusion of blend compressibility is essential for treating the important pressure dependence[3] of multicomponent polymer systems. In contrast, FH and many other theories ignore compressibility, an assumption that often is justified by internal consistency, i.e., because the theory is found to "work". However, the presence of a nontrivial equation of state for polymers in the liquid state implies that the systems are indeed compressible, although some phenomena may be analyzed adequately[15] with an incompressible model. For instance, the incompressibility assumption is often invoked in the low frequency, long wavelength limit of hydrodynamics, even though this approximation incorrectly predicts an

S0024-9297(98)00702-5 CCC: $15.00
Published on Web 09/03/1998

infinite speed of sound. Some controversy has surrounded the question of the appropriateness of the incompressibility approximation for analyzing small angle neutron scattering (SANS) data for polymer blends. For example, Joanny and Benoit[16] cite the well-known[17] separation of contributions from composition and density fluctuations to the extrapolated foward scattering SANS intensities as support for the argument that blend compressibility may be ignored in analyzing SANS data. However, their expressions for the contribution to the forward scattering SANS intensity from composition fluctuations contain thermodynamic derivatives at constant pressure, derivatives that are *undefined in an incompressible model*. Moreover, the observed pressure dependence of coherent scattering intensities from polymer blends indicates a strong limitation of the incompressibility approximation.[18,19] On the other hand, the greater complexity posed by introducing compressibility into the theory often renders the consideration of the (high pressure) incompressible limit as a useful first approximation and as a vehicle for understanding certain general trends.

The theoretical description of a compressible binary blend (with a theory, such as a compressible generalization[20] of FH theory, Sanchez−Lacomb theory,[21] the Flory−Orwoll−Vrij[22] equation of state theory, the LCT, etc.[23]) requires, at minimum, the specification of three interaction parameters. Two homocontact interaction parameters may be determined from thermodynamic data for the pure homopolymer melts, while the heterocontact parameter is often fit to blend data, such as SANS χ parameters, phase diagrams, etc. This fitting of three interaction parameters is a process of considerably greater complexity than the application of an incompressible model which contains a single interaction parameter. Thus, bearing in mind the limitations of incompressible models, we consider here the high molecular weight, incompressible limit of the LCT in order to elucidate general trends in polymer blend thermodynamics and to provide far more compact and readily usable expressions for generating initial approximations for use with the compressible LCT. This incompressible limit of the LCT has already been used[13] to identify the various *molecular* factors responsible for the enhanced miscibility of poly(ethylene propylene) with head-to-head poly(propylene) than with atactic poly(propylene).[14] Several trends derived from the incompressible model agree well with those obtained by using the full LCT for compressible systems.

Section II briefly sketches some essential aspects of the extended lattice model of structured monomers and describes the physical motivations underlying the approximations invoked by the LCT. A detailed table presents the entropic structural parameters (ESP) that appear in the final LCT free energy expressions, thereby enabling rapid use of the theory for a wide variety of monomer molecular structures. The table summarizes the ESP for purely flexible polymer molecules, and the extension to include chain semiflexibility will be given elsewhere. (Some applications of the semiflexible chain theory, however, are quoted here and in ref 13.) Section III provides surprisingly simple analytical expressions for the LCT free energy of mixing and for the LCT SANS χ parameter of a binary polymer blend in the high molecular weight, incompressible limit. Emphasis is placed on the molecular features affecting the χ parameter and blend miscibilities. In particular, we study how

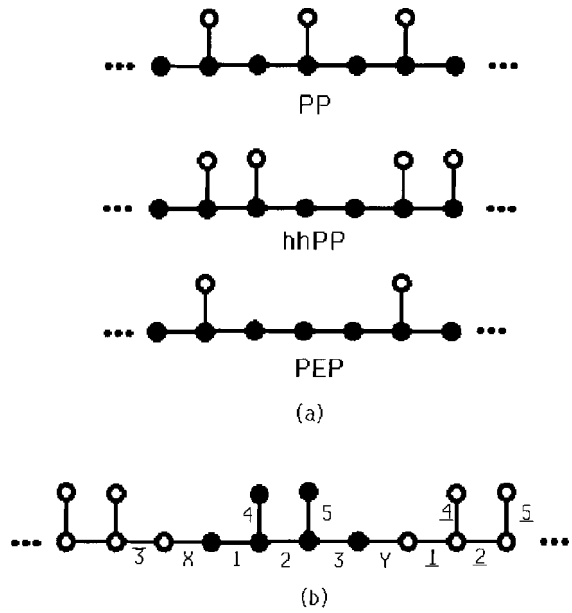

Figure 1. (a) Portions of polypropylene (PP), head-to-head polypropylene (hhPP), and poly(ethyl propylene) (PEP) chains with monomers represented by united atom structures. Individual CH_n ($n = 0-3$) groups occupy single lattice sites and are denoted by circles. Filled circles represent backbone chain united atom groups, while open circles indicate the side groups. (b) A portion of a hhPP chain with the central monomer (filled circles) and two neighboring units (open circles). Bonds on the central and neighboring monomers are labeled, respectively, as {1, 2, 3, 4, 5}, {$\bar{3}$}, and {$\underline{1}$, $\underline{2}$, $\underline{4}$, $\underline{5}$}. X and Y label the connecting bonds between the central monomer and its neighbors.

monomer molecular structures influence the "entropic χ", the probabilities of monomer-monomer contacts, and nonrandom mixing effects. Section IV then applies the theory to explain the prevalence of lower critical solution temperature phase diagrams in blends of poly(isobutylene) with other polyolefins. The section continues with probing the molecular reasons why many polyolefin blends exhibit a rather large negative "entropic χ" parameter A. The analysis indicates the strong influence of chain stiffness on miscibility of weakly interacting polyolefin blends and thereby impacts on the Bates−Fredrickson[24] model for polyolefin miscibilities.

II. Extended Lattice Model and LCT

The extended lattice model of polymer systems[3−5] is constructed from the standard lattice model by allowing monomers to cover several lattice sites. The bonds between submonomer units mimic the connectivities in the actual monomer structures as far as permitted by the lattice structure. For example, when applied to polyolefin chains, individual CH_n groups ($n = 0, ..., 3$) units are taken to occupy single lattice sites as shown in Figure 1a which depicts several examples of polyolefin united atom structures. Filled circles in Figure 1a designate united atom groups on the chain backbone, while open circles denote the side groups. Bonds connecting the united atom units represent the carbon−carbon bonds in the actual polyolefins. No two united atom groups may lie on the same lattice site, and united atom groups of species α and β on neighboring lattice sites interact with the attractive van der Waals energy $\epsilon_{\alpha\beta}$. Extensions of the model to describe chain semiflexibility[25] require the specification of energy differences $E_b^{(\alpha)}$ between "trans" and "gauche" confor-

mations for two consecutive bonds on chains of species α, where "trans" bonds are collinear, while "gauche" bonds lie along orthogonal directions. The incompressible limit constrains all excess thermodynamic properties of binary blends to depend[26] only on a single exchange energy

$$\epsilon = \epsilon_{AA} + \epsilon_{BB} - 2\epsilon_{AB} \tag{1}$$

thereby reducing the number of independent interaction parameters from three for a compressible binary blend to one for an incompressible model system. This presence of a single interaction energy parameter provides one strong motivation behind the wide spread preference for using incompressible system models.

The partition function for the extended lattice model is evaluated within the LCT by introducing approximations for the bonding constraints and for the excluded volume and van der Waals interactions. The excluded volume interactions are represented in the lattice model by the condition that no two united atom groups can occupy the same lattice site. The partition function W_p for the packing of polymer chains on the lattice contains the Boltzmann factor $\exp[-\beta\sum_i U_{bond}(\mathbf{r}_{i-1} - \mathbf{r}_i)]$, where $U_{bond}(\mathbf{r}_{i-1} - \mathbf{r}_i)$ is the potential energy describing the chemical bond between the united atom units $i-1$ and i. This Boltzmann factor simplifies enormously in the lattice model to the constraint that the vector $\boldsymbol{r}_{i-1} - \boldsymbol{r}_i$ connecting these units is one of the lattice vectors $\mathbf{a}_\beta$ ($\beta = 1, ..., z$) between nearest neighbor sites, where z is the number of nearest neighbors to any lattice site. The above simplification may be written as

$$\exp[-\beta U_{bond}(\mathbf{r}_{i-1} - \mathbf{r}_i)] \rightarrow \sum_{\beta=1}^{Z} \delta(\mathbf{r}_{i-1} - \mathbf{r}_i - \boldsymbol{a}_\beta) \tag{2}$$

where δ is the Kronecker "delta" function and the sum over β appears because the bond may lie along any of z possible directions.

The approximate treatment of the bonding constraints in eq 2 may be motivated by recourse to the "Flory theorem" which states that in polymer melts we cannot discern whether nonbonded nearest neighbor united atom groups belong to different polymer chains or to distant portions of the same polymer molecule.[1] Thus, in melts, the excluded volume prohibition of multiple occupancy of a site is more important than the long-range consequences of the bonding constraints. On the basis of the Flory theorem, we introduce the zeroth order mean-field average $A = \langle \delta(\mathbf{r}_{i-1} - \mathbf{r}_i - \mathbf{a}_\beta) \rangle$ of the bonding constraints to re-express eq 2 exactly as

$$\sum_{\beta=1}^{Z} \delta(\mathbf{r}_{i-1} - \mathbf{r}_i - \boldsymbol{a}_\beta) \equiv zA(1 + X_{i-1,i}) \tag{3}$$

with the bond correlation factor $X_{i-1,i}$ given as

$$X_{i-1,i} = (zA)^{-1} \sum_{\beta=1}^{Z} \delta(\mathbf{r}_{i-1} - \mathbf{r}_i - \boldsymbol{a}_\beta) - 1 \tag{4}$$

The overall bonding Boltzmann factor for the whole system is the product (over all bonds in the system) of individual terms of the form in eq 3. Therefore, eq 3 can be written for specified positions of the united atom groups as

$$\prod_{bonds} \exp[-\beta U_{bond}(\mathbf{r}_{i-1} - \mathbf{r}_i)] = \prod_{bonds} [zA(1 + X_{i-1,i})] \tag{5}$$

The athermal limit partition function W_p is computed by summing eq 5 over all possible positions of the united atom units subject to the strict excluded volume constraints. The product over bonds [on the right-hand side of eq 5] generates a cluster expansion for the partition function W_p in the athermal limit ($T \rightarrow \infty$). The average quantity A may be chosen such that the leading zeroth order contribution generates the Flory combinatorial entropy, while the $X_{i-1,i}$ terms introduce nonrandom mixing corrections (including a noncombinatorial entropy) arising from the correlations introduced by the presence of bonds. Our previous papers[4,25b] describe the rather complicated details involved in evaluating these corrections and summarize their values in terms of monomer structure dependent counting indices described below.

The cluster expansion, generated from eq 5, yields the free energy as an series in powers of $1/z$, while a similar treatment of the van der Waals interactions produces the remaining contributions to the free energy as double expansions in $1/z$ and $\epsilon_{\alpha\beta}/kT$. The athermal and order $\epsilon_{\alpha\beta}$ portions have been evaluated through order $1/z^2$, while the order $(\epsilon_{\alpha\beta})^2$ contributions are only available through order $1/z$. The truncation of the series in $\epsilon_{\alpha\beta}/kT$ implies that the LCT applies only in the range of higher temperatures. As noted above, the LCT excess free energy in the incompressible limit depends on the interaction energies only through the single dimensionless exchange energy ϵ/kT. Since ϵ/kT for polymer blends is typically of order 10^{-2} (or less) per united atom group, the expansion of the LCT free energy series in ϵ/kT may safely be truncated at order $(\epsilon/kT)^2$.

The dependence on monomer molecular structures enters the LCT free energy through a series of counting indices[4,5] $N_\alpha^{(i)}$ which enumerate the number of distinct sets of i sequential bonds in a chain of species α. The only coefficients, appearing in the LCT expression for the free energy of mixing for a homopolymer blend (see section III), are[25b] the ratios of $N_\alpha^{(2)}/M_\alpha$ and $N_\alpha^{(3)}/M_\alpha$ where M_α is the number of united atom groups in a whole polymer chain of species α. The former may be represented more conveniently (by using Euler relations[27]) in terms of the respective numbers $s_\alpha^{(tri)}$ and $s_\alpha^{(tetra)}$ of tri- and tetrafunctional united atom groups in a single monomer[28] of species α as[29]

$$r_\alpha \equiv \frac{N_\alpha^{(2)}}{M_\alpha} = 1 + \frac{s_\alpha^{(tri)}}{s_\alpha} + 3\frac{s_\alpha^{(tetra)}}{s_\alpha} \tag{6a}$$

where s_α designates the number of united atom units in an α species monomer and where the large M_α limit has been invoked.

The evaluation of r_α is now illustrated for the three polyolefin structurs in Figure 1a. None of the polyolefins in Figure 1a contains tetrafunctional groups, so $s_\alpha^{(tetra)}/s_\alpha = 0$ for all three structures. Only one of the three united atom groups of the PP monomer is trifunctional. Thus, we get $s_{PP}^{(tri)}/s_{PP} = 1/3$ and $r_{PP} = 4/3$. The hhPP chain has six united atom groups per monomer, two of which are trifunctional, and, therefore, $r_{hhPP} = 1 + 2/6$, which equals r_{PP}. Similar counting for a PEP monomer yields $r_{PEP} = 6/5$. The extension of eq 6a to

describe semiflexible polymers emerges in the form[25]

$$r_\alpha \equiv \frac{N_\alpha^{(2)}}{M_\alpha} = \left[1 - \frac{s_\alpha^{(\mathrm{tri})}}{s_\alpha} - 3\frac{s_\alpha^{(\mathrm{tetra})}}{s_\alpha}\right] g_\alpha + 2\left[\frac{s_\alpha^{(\mathrm{tri})}}{s_\alpha} + 2\frac{s_\alpha^{(\mathrm{tetra})}}{s_\alpha}\right] \quad (6b)$$

where

$$g_\alpha = z/[z - 1 + \exp(E_b^{(\alpha)}/kT)] \quad (6c)$$

with $E_b^{(\alpha)}$ the trans-gauche energy difference for species α.

While the counting for $N_\alpha^{(3)}$ can be simplified by using Euler relations for certain cases,[30] the simplification does not apply, for example, to the three polyolefin chains depicted in Figure 1a because they contain methyl side groups. Therefore, the geometrical index $N_\alpha^{(3)}$ is evaluated by directly enumerating all sets of three sequential bonds that traverse a single monomer of species α. We illustrate this process for the case of the hhPP chain in Figure 1b, which depicts a central monomer with its united atom units designated by filled circles and with the bonds labeled as 1, 2, 3, 4, and 5. The figure also contains portions of the neighboring monomers which are distinguished by representing their united atom units by open circles and their bonds as $\bar{3}$ and $\underline{1}$, etc. The bonds labeled X and Y connect the central monomer to its neighbors. The *distinct* sequences of three successive bonds that contain at least one bond belonging to the central monomer are the bond sequences 123, 125, 1X$\bar{3}$, 21X, 23Y, 3Y$\underline{1}$, 324, 41X, 425, and 53Y. The bond sequences with a bond lying entirely on a neighboring monomer, such as 1X$\bar{3}$ and 3Y$\underline{1}$, are counted with a weight factor of $^1/_2$, while the remaining sequences are counted with unit weights. Thus, the direct counting gives $N_{\mathrm{hhPP}}^{(3)} = 8 + 2(1/2)$ which corresponds to nine runs of three bonds per hhPP monomer. Since each hhPP monomer contains six united atom groups, we obtain $p_{\mathrm{hhPP}} \equiv N_{\mathrm{hhPP}}^{(3)}/M_{\mathrm{hhPP}} = 9/6$. Reference 25 presents more details of computing $N_\alpha^{(3)}$ for semiflexible chains, and we defer to a future work more extensive applications of the semiflexible chain theory.

Table 1 presents the ratios r_α and p_α (in the long chain limit) for the numerous examples of monomer structures depicted in Figure 2. Both r_α and p_α are written in Table 1 as fractions, where the denominators are the numbers s_α of lattice sites occupied by individual monomers, while the numerators provide the quantities $N_\alpha^{(2)}$ and $N_\alpha^{(3)}$ per monomer, respectively. This notation better illustrates the simplicity of the counting techniques, thereby enabling straightforward application to other structures. Filled circles in Figure 2 represent backbone united atom units, while open circles correspond to side group units. Dashed horizontal lines designate the bonds to neighboring monomers, while vertical dashed lines with arrows (in structures f–j) indicate that the side group contains $k \geq 2$ or $m \geq 2$ united atom units with the delineated connectivities.

Table 1. Geometrical Coefficients r_α and p_α for Various Polymers α Whose United Atom Monomer Structure Models Are Depicted in Figure 2

monomer structure in Figure 2	r_α	p_α
a	2/2	2/2
b	4/3	4/3
c	6/5	6/5
d	4/3	9/6
e	7/4	6/4
f[a]	$(3 + k)/(2 + k)$	$(4 + k)/(2 + k)$
g[a]	$(5 + k)/(4 + k)$	$(6 + k)/(4 + k)$
h[a]	$(4 + k)/(3 + k)$	$(5 + k)/(3 + k)$
i[a]	$(6 + k)/(3 + k)$	$(7 + k)/(3 + k)$
j[b]	$(5 + k + m)/(2 + k + m)$	$(8 + k + m)/(2 + k + m)$
k	7/5	8/5
l	5/3	5/3
m	16/9	19/9
n	4/3	5/3
o	10/7	12/7
p	9/7	14/7
q	11/8	12/8
r	11/7	13/7
s	13/8	16/9
t	11/8	14/8
u	13/9	16/9

[a] Valid for $k \geq 2$. [b] Valid for $k \geq 2$ and $m \geq 2$.

III. High Molecular Weight, Incompressible Limit for SANS χ

Let $\varphi = \varphi_1 = 1\text{-}\varphi_2$ designate the composition of a binary blend and N_l be the total number of lattice sites. The free energy of mixing ΔF^{mix} for a binary blend in the high molecular weight, incompressible limit is obtained,[31] after some algebra, as

$$\frac{\Delta F^{\mathrm{mix}}}{N_l kT} = \frac{\varphi}{M_1}\ln\varphi + \frac{1-\varphi}{M_2}\ln(1-\varphi) + \varphi(1-\varphi)\left\{\frac{(r_1 - r_2)^2}{z^2} + \left(\frac{\epsilon}{kT}\right)\left(\frac{z-2}{4} - [p_1(1-\varphi) + p_2\varphi]\right) - \varphi(1-\varphi)\left(\frac{\epsilon}{kT}\right)^2\left(\frac{z+2}{4} + r_1(1-\varphi) + r_2\varphi\right)\right\} \quad (7)$$

in terms of the notation $r_\alpha = N_\alpha^{(2)}/M_\alpha$ and $p_\alpha = N_\alpha^{(3)}/M_\alpha$. The first two terms on the right-hand side of eq 7 represent the usual configurational entropy, while the contribution $\varphi(1-\varphi)(r_1 - r_2)^2/z^2$ is the noncombinatorial entropy of mixing, which stems from the local correlations associated with the packing of monomers with different sizes and shapes. This term arises because the Flory treatment overcounts disallowed configurations, such as ones where one pair of successive bonds on a chain completely overlaps a pair of successive bonds on another and where the end units on two sets of pairs of sequential bonds lie on the same lattice sites (with the four bonds forming a square configuration on cubic lattices), etc. The two remaining terms in eq 7 are of energetic origin and contain both monomer structure dependent and independent contributions as discussed further below. Of particular note is the fact that the ϵ^2 term is negative definite and therefore stabilizes the blend miscibility.

The incompressible limit SANS χ parameter is defined in terms of the free energy of mixing ΔF^{mix} through

$$\frac{\partial^2(\Delta F^{\mathrm{mix}}/N_l kT)}{\partial\varphi^2} = \frac{1}{M_1\varphi} + \frac{1}{M_2(1-\varphi)} - 2\chi_{\mathrm{site}} \quad (8)$$

where the subscript *site* on χ_{site} indicates that the χ parameter is defined *per lattice site*. The usual experimental definition of χ is written in term of the extrapo-

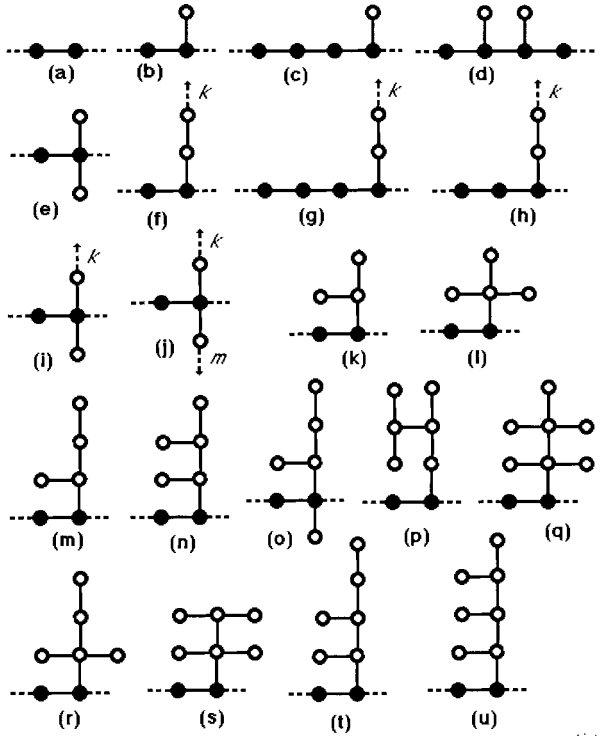

Figure 2. United atom monomer structure models whose structural parameters s_α, r_α, and p_α are given in Table 1. Filled circles denote monomer portions lying on the chain backbone, while open circles represent those belonging to the side groups. Dashed horizontal lines designate the bonds to neighboring monomers, and vertical lines with arrows and symbols *k* (or *m*) indicate that a given monomer has *k* (or *m*) united atom side group units connected as illustrated.

lated forward coherent scattering $I(0)$ as

$$\chi_{\text{expt}} = \left(\frac{v_0}{2}\right)\left[\frac{1}{N_1 v_1 \varphi_1} + \frac{1}{N_2 v_2 \varphi_2} - \frac{k_N}{I(0)}\right] \tag{9}$$

where N_α and v_α are the polymerization index and the molar monomer volume of species α, respectively, $v_0 = (v_1 v_2)^{1/2}$, and $k_N = N_0(b_1/v_1 - b_2/v_2)^2$, with b_α being the monomer scattering length and N_0 being Avogadro's number. Equation 9 defines χ_{expt} on a *per monomer* basis. Hence, the comparison of the LCT χ_{site} with the experimental χ_{exp} requires the determination of a conversion factor which is derived in the appendix for an arbitrary binary blend. (Recall that the exchange energy ϵ of eq 1 is likewise defined in the LCT on a per lattice site basis.)

The general relation between χ_{site} and χ_{exp} in eq A9 simplifies when the ratio $s = s_1/s_2$ of monomer occupancy indices s_1 and s_2 for the two blend components coincides with the ratio $v = v_1/v_2$ of the specific monomer volumes. United atom models of polyolefin blends automatically satisfy this equality between s_1/s_2 and v_1/v_2 (under the simplifying assumption of common densities for both components), and LCT monomer molecular structures are generally chosen to reproduce this equality as closely as possible. Therefore, the theoretical χ_{site} of eq 8 and the experimental χ_{exp} of eq 9 are related to each other by the simple expression

$$\chi_{\text{exp}} = (s_1 s_2)^{1/2}\chi_{\text{site}} \tag{10}$$

Applying the high molecular weight limit $M_1, M_2 \to \infty$ to the free energy derivative in eq 8 converts χ_{site} into the simple polynomial

$$\chi_{\text{site}} = \frac{1}{z^2}(r_1 - r_2)^2 + \left(\frac{\epsilon}{kT}\right)\left(\frac{z-2}{2} + \frac{1}{z}\{p_1[1 - 3(1 - \varphi)] + p_2(1 - 3\varphi)\}\right) + \left(\frac{\epsilon}{kT}\right)^2\left(\frac{(z+2)[1 - 6\varphi(1-\varphi)]}{4} + r_1(1-\varphi)(1 - 8\varphi + 10\varphi^2) + r_2\varphi(3 - 12\varphi + 10\varphi^2)\right) \tag{11}$$

The first term on the right-hand side of eq 11 is the athermal limit entropic component of χ_{site} which depends on the monomer structures of the two blend components. We have previously shown[29] that the entropic structural parameter $r = |r_1 - r_2|$ correlates well with the computed critical temperature for compressible binary blends when all interaction energies are equal, i.e., when $\epsilon_{11} = \epsilon_{22} = \epsilon_{12}$. The remaining contributions to χ_{site} in eq 11 are of energetic origin. The leading energetic contribution of $z\epsilon/2kT$ is merely the Flory−Huggins interaction term that grossly overestimates the number of nearest neighbor heterocontacts.[32,33] The replacement of the factor of z in the FH approximation $z\epsilon/2kT$ by $z - 2$ is consistent with the arguments of Guggenheim[34] that each interior unit in a linear chain is linked by chemical bonds to two nearest neighbor units. Consequently, these two neighboring sites are unavailable for heterocontact interactions with units belonging to the other species. The second term of order ϵ/kT provides a correction to the number of heterocontacts due to the packing constraints imposed by the monomer molecular structures. This last term contains both composition-dependent and -independent portions. The composition-dependent part provides a correction to the random mixing approximation (in the strict probabilistic sense).[35] A portion of the composition-dependent order ϵ/z terms in eq 11 reduces for linear chains to the order $1/z$ contributions from Guggenheim counting (in the high molecular weight limit). The $(\epsilon/kT)^2$ contributions in eq 11 contain additional nonrandom mixing terms which depend on composition and monomer structures.

The appearance of the counting indices p_α in the coefficient of ϵ in eq 11 represents a generalization of the mathematically rather vague Guggenheim "surface fraction" concept to structured monomers as follows: Consider a sequence of three consecutive bonds on a chain (even on a linear chain). When these three bonds occur in a U-shaped conformation on cubic lattices, each of the two end units in the three-bond sequence has an additional nearest neighbor on the same chain. Consequently, for this three-bond U-shaped configuration, one less neighboring lattice site is available to the end united atom groups for heterocontact interactions. Clearly, one higher order term of this variety emerges as proportional to $(\epsilon/kT)(N_\alpha^{(5)}/zM_\alpha)$. These considerations emphasize that the vague concept of "surface fractions" is automatically quantified and extended to structured monomers by the LCT, and the proper computation of surface fractions involves complicated averages over chain conformations.

The stability limit for the occurrence of a single homogeneous phase is defined by the vanishing of the second derivative in eq 8

$$\frac{1}{M_1\varphi} + \frac{1}{M_2(1-\varphi)} - 2\chi_{\text{site}} = 0 \tag{12}$$

The solution of the resulting equation produces the spinodal temperature T_s as a function of composition φ, molecular weights M_α, and monomer structures. Recalling that ϵ is defined per lattice site, the dimensionless ratio ϵ/kT_s is generally very small (less than 10^{-2}). Consequently, it often suffices to retain only the linear contributions in ϵ/kT from eq 11 as

$$kT_s/\epsilon = \frac{\left\{z - 2 + \left(\frac{2}{z}\right)\{p_1[1 - 3(1-\varphi)] + p_2(1 - 3\varphi)\}\right\}}{\left\{\frac{1}{M_1\varphi} + \frac{1}{M_2(1-\varphi)} - 2\frac{(r_1 - r_2)^2}{z_2}\right\}} \tag{13}$$

The presence of the athermal limit entropic portion of χ_{site} in the denominator of eq 13 indicates the possibility of generating a lower critical solution temperature (LCST) when the exchange energy ϵ is attractive (i.e., $\epsilon < 0$) and when the disparities in monomer structures between the two blend components are sufficiently large to satisfy the inequality

$$2\frac{(r_1 - r_2)^2}{z^2} > \frac{1}{M_1\varphi} + \frac{1}{M_2(1-\varphi)} \tag{14}$$

This monomer structure driven mechanism[24a] for the occurrence of a LCST phase diagram differs from the one conventionally invoked. The traditional mechanism explains the growth of an unfavorable entropy of mixing with increasing temperature as a consequence of a difference in the thermal expansion coefficients between the two components of a compressible binary system. The present structural mechanism for a LCST predicts[24a] a much weaker variation of the critical temperature with molecular weights than is common for systems with upper critical solution temperature (UCST) phase diagrams, a feature found for blends of poly(isobutylene) with other polyolefins.[36] As mentioned above, the numerator in eq 13 introduces a correction to the Flory–Huggins number (z) of neighbor contacts due to local chain connectivities (the correction, in turn, depends on monomer structure and composition.) Using the full expression for χ_{site} [see eq 10] in the spinodal condition of eq 12 generates, in principle, two solutions, one of which is generally and quite clearly extraneous. However, all the LCT analyses of polyolefin blends studied to date display values for ϵ/kT that are sufficiently small to permit neglecting the order ϵ^2 contributions. Consequently, dropping the order ϵ^2 terms leads to only one spinodal temperature and the absence of the obviously unphysical extraneous solution.

IV. Applications of Incompressible LCT

A. LCST Polyolefin Blends. Binary blends of poly(isobutylene) (PIB) with other polyolefins represent typical examples of polyolefin systems that exhibit[36] large negative values of the SANS χ_{exp} parameter and a lower critical solution temperature (LCST) phase diagram. This LCST behavior departs significantly from that observed for the majority of binary polyolefin blends, and moreover, the LCST polyolefin blends are of considerable interest because their thermodynamic properties cannot be explained by solubility parameter theory which has been applied successfully to a number of polyolefin blends by Graessley et al.[14] Thus, the thermodynamic description of these LCST blends of PIB presents a significant challenge to any polymer theory concerned with describing the molecular factors controlling blend miscibility. Consequently, these PIB blends are analyzed here with the high pressure, high molecular weight limit of the LCT in order to illustrate the predictive abilities of this simplified version of LCT.

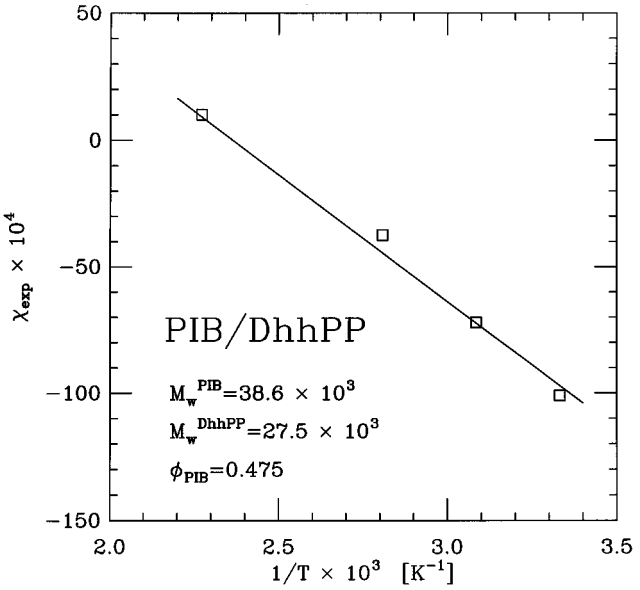

Figure 3. Comparison of the calculated and experimental SANS χ_{exp} parameter for PIB/DhhPP blends as a function of the inverse temperature. Squares are the experimental data of Krishnamoorti et al.[36] for φ(PIB)=0.475, while the solid line is a least-squares fit of LCT eqs 10 and 11 for $\epsilon = -1.16$ K. The experimental molecular weights are indicated on the figure.

Since the incompressible limit of the theory implies the neglect of blend compressibility, only one independent energy, ϵ, appears as an adjustable parameter in calculations based on eqs 10 and 11. After this empirical value of ϵ is introduced, all remaining quantities in these equations (i.e., r_α and p_α) are determined from the united atom monomer structures in Figure 2 by elementary counting (see Table 1). Figure 3 compares the calculated and experimental SANS χ_{exp} parameters for poly(isobutylene)/head-to-head polypropylene (PIB/DhhPP) blends as a function of the inverse temperature. Squares denote the experimental data of Krishnamoorti et al.[36] for $\varphi_{PIB} = 0.475$, while the solid line is obtained from a least-squares fit for $\epsilon = -1.16$ K (per lattice site) of the LCT eqs 10 and 11. (The united atom monomer structures for PIB and hhPP are depicted by diagrams e and d of Figure 2, respectively.) The least-squares fit guarantees that the theory reproduces the slope of χ_{exp} vs $1/T$, but the remarkable feature of Figure 3 is the excellent theoretical representation for the entropic portion of χ_{exp}.

Given the empirical value for ϵ, the LCT immediately provides predictions for the composition dependence of the SANS χ parameter which to our knowledge has not yet been studied. This composition dependence is illustrated for two different temperatures in Figure 4. The squares correspond to the experimental data that are available only for the single composition $\varphi_{PIB} = 0.475$. The convex parabolic variation of $\chi(\varphi)$ for PIB blends in Figure 4 becomes less pronouced at higher temperatures, almost disappearing, for instance, at 167 °C.

Figure 5 further explores the influence of monomer molecular structures on the miscibility of PIB blends by presenting spinodal curves for three binary blends

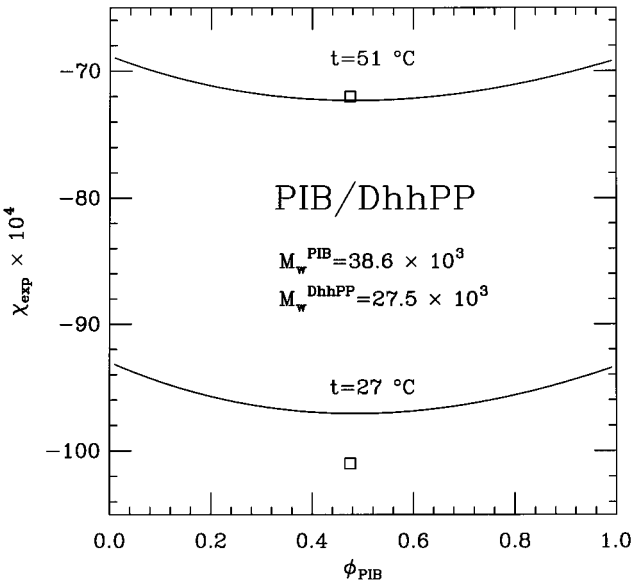

Figure 4. LCT predictions for the composition dependence of the interaction parameter χ_{exp} at t = 27 °C and 51 °C for PIB/DhhPP blends. Squares are experimental data from ref 36. The exchange energy $\epsilon = -1.16$ K is taken from the fit in Figure 3.

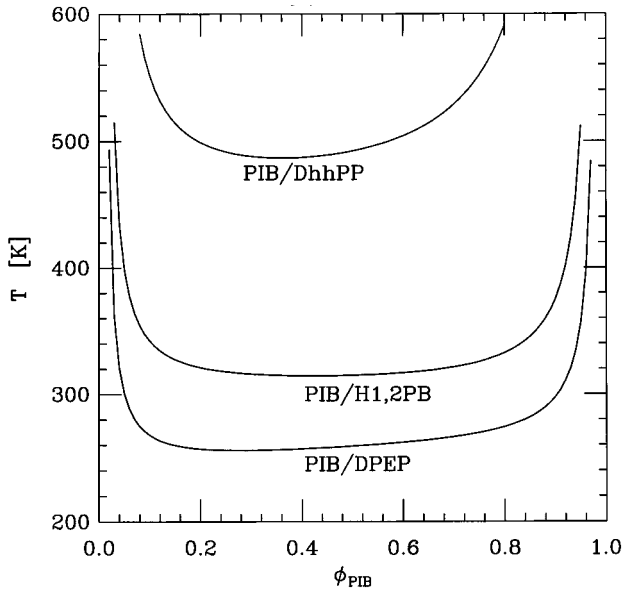

Figure 5. Spinodal curves for PIB/DhhPP, PIB/H1,2PB, and PIB/DPEP blends generated from the LCT by using a common value $\epsilon = -1.16$ K for all three systems. The molecular weights corresponds to experimental samples studied by Krishamoorti et al.[36]

of PIB with other polyolefins. The "homologous" nature of the second component leads us to use the same PIB/DhhPP exchange energy $\epsilon = -1.16$ K for all three systems. The computed phase diagrams (in Figure 5) accord with the experimental observations[36] that PIB/DhhPP is a strongly miscible system, whereas mixtures of PIB with both poly(ethyl propylene) (PEP) and saturated 1,2-polybutadiene (H1,2PB) are phase separated at room temperatures. The computed critical temperature T_c for the PIB/H1,2PB blend is higher by at least 20 K than the T_c deduced from the visual observation[36] of cloud points for the PIB/D97 system, a small difference considering the use of the same exchange energy ϵ as determined for PIB/DhhPP mixtures. Experiments find that a 50−50 mixture of PIB and

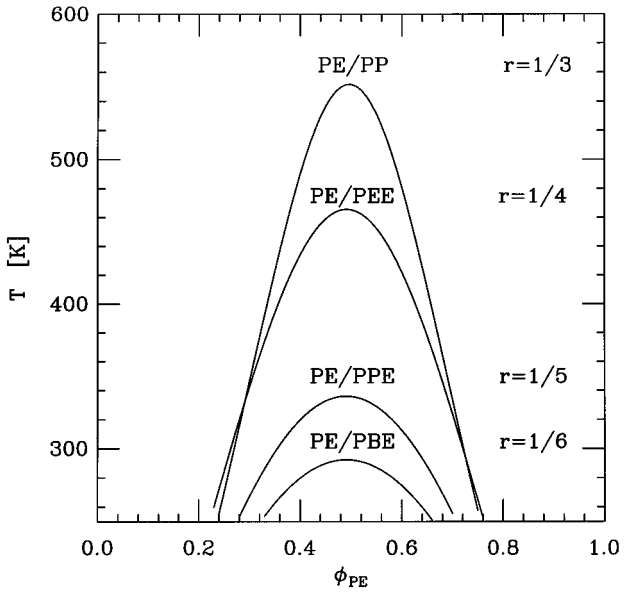

Figure 6. LCT predictions of spinodal curves for a series of blends having PE as a common component. The numbers of carbon atoms M_1 and M_2 for the two blend species are assumed to be identical for the PE/PBE, PE/PPE, and PE/PEE systems ($M_1 = M_2 = 600$), but are slightly lower ($M_1 = M_2 = 450$) for the PE/PP blends. The use of lower $M_1 = M_2 = 450$ keeps the computed critical temperature within physical bounds. All four curves are generated for a common value of exchange energy $\epsilon = +0.415$ K to illustrate the influence of monomer molecular structures on the blend miscibilities. The trend in miscibilities is consistent with the values of blend entropic parameter r given in the figure.

DPEP is phase separated at 298 K, whereas the computed spinodal temperature in Figure 5 is 260 K, again indicating good agreement.

Prior LCT computations demonstrate[29] that when both components in a binary blend are energetically very similar, the trends in blend miscibility can be predicted by the entropic structural parameter (ESP) $r = |r_1 - r_2|$. The ESPs for the PIB/DhhPP, PIB/H1,2PB, and PIB/DPEP mixtures are readily evaluated using Table 1 and Figure 2 as 5/12, 1/2, and 11/20, respectively. The relative ordering of these three ESPs is consistent with the declining miscibility, i.e., with a decreasing critical temperature for these three systems. A smaller ESP r implies a smaller χ (when the exchange energy is rather small) and, in turn, an improved blend misciblity. A similar pattern emerges from our LCT calculations for UCST polyolefin blends, as illustrated in Figure 6. The spinodal curves for all four binary blends of PE with other polyolefins are likewise computed by using the same exchange energy $\epsilon = +0.415$ K per united atom group. Hence, the computed miscibility disparities for these systems stem solely from different degrees of structural asymmetry between the two blend components.

B. Polyolefin Blends with UCST Phase Diagrams. The extensive SANS studies binary polyolefin blends by Graessley, Lhose, and co-workers[14,36] yield numerous examples of systems exhibiting UCST phase diagrams. Confining attention to those cases where χ_{exp} is observed to vary as $\chi_{exp} = A + B/T$, we are struck by the many examples where A is large and negative. (Indeed $|A|$ is often comparable to B/T and χ_{exp}.) Clearly, the incompressible limit expression for the temperature independent portion of χ_{exp} [see eq 11] cannot produce a negative A. This feature of the LCT stems from the

fact that the Flory−Huggins approximation, of necessity, overcounts configurations that are disallowed by excluded volume constraints. Several possible reasons might account for this perplexing behavior, as follows.

(a) Many samples involve random copolymers for which eq 11 does not apply.

(b) The partially deuterated samples may contain a nonuniform distribution of deuterium among the monomers that can be a source of additional fluctuations that enhance the neutron scattering.

(c) The systems are compressible as evidenced by their nontrivial equations of state.

(d) The two blend species exhibit different measures of stiffness which, as emphasized by Bates and Fredrickson[24] and others,[13,25,37] can influence miscibility patterns.

It is, of course, possible that the observed behavior arises from a combination of the four molecular factors, but a natural first analysis considers each factor individually. To eliminate explanation a, we focus on the system of PP/hhPP which almost conforms to a binary homopolymer blend (i.e., the microstructural randomness is quite small). We are currently unable to assess possibility b and, therefore, defer its treatment to a future date. Passing on to case c, a large number of LCT computations indicate that just including compressibility is insufficient to produce a large negative A, thereby eliminating mechanism c as the *sole* reason. Thus, we are left with chain semiflexibility as a possible sole source for the large negative A found for PP/hhPP binary blends.

The extension of eq 11 to semiflexible polymers[13,25] merely requires introducing a dependence of the parameters r_α and p_α on the trans-gauche energy difference $E_b^{(\alpha)}$. The r_α and p_α emerge for PP and hhPP in the form

$$r_\alpha = \frac{2}{3}(g_\alpha + 1), \quad \alpha = \text{PP or hhPP} \tag{15a}$$

$$p_\alpha = \frac{2}{3} g_\alpha [g_\alpha + 1], \quad \alpha = \text{PP} \tag{15b}$$

$$p_\beta = \frac{2}{3}\left[g_\beta^{\,2} + g_\beta + \frac{1}{4}\right], \quad \beta = \text{hhPP} \tag{15c}$$

where the weight factors g_α depend on the respective energies $E_b^{(\alpha)}$ as given in eq 6c. Notice that the dependence of r_α and p_α on chain stiffness emerges in the LCT through a temperature dependent factor in contrast to the primarily athermal nature of its representation in the Bates-Fredrickson model.[24]

Before describing the comparison of the semiflexible chain LCT with the data for PP/hhPP binary blends, we note another feature of the experimental data that is equally perplexing when viewed on a microscopic scale. Fitting the experimental data for χ of PP/DhhPP to the empirical form of $A + B/T$ yields the large negative $A = -4.46 \times 10^{-3}$ and $B = 2.38$ K (per monomer unit). This value for B is comparable to those corresponding to moderately immiscible UCST polymer blends, in sharp contrast to expectations that the chemically almost identical PP and hhPP chains should have a nearly vanishing exchange energy. Thus, we consider whether the semiflexible LCT theory can likewise explain the molecular origins of the large B for PP/DhhPP.

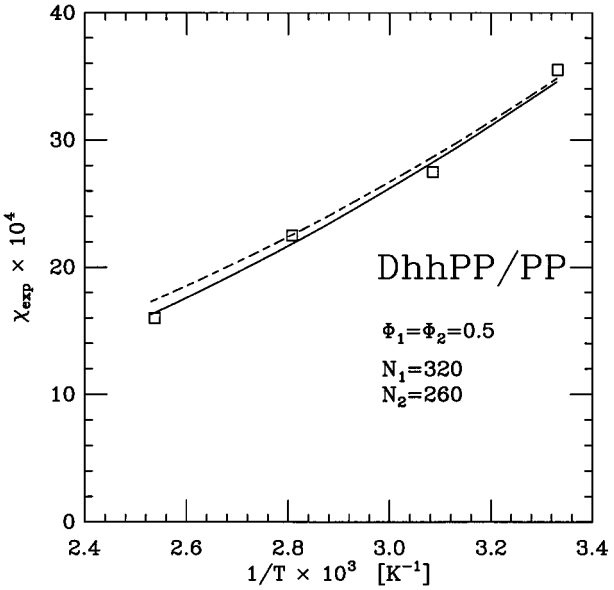

Figure 7. Comparison of the calculated and experimental SANS χ_{exp} parameter for DhhPP/PP blends as a function of the inverse temperature. Squares denote the experimental data of Krishnamoorti et al.[36] for a 50−50 composition mixture. Both solid and dash lines represent LCT fits with different values of exchange energy ϵ and the bending energies E_b(hhPP) and E_b(PP). ($\epsilon = -0.0166$ K, E_b(hhPP) = 498 K, and E_b(PP)=208 K for the solid line and $\epsilon = +0.000415$ K, E_b(hhPP) = 419 K, and E_b(PP) = 125 K for the dashed line). The experimental polymerization indices N_1 and N_2 are listed in the figure.

Equations 11 and 15 predict that the slope of χ_{exp} vs $1/T$ is dominantly, but not entirely, determined by the magnitude of the exchange energy ϵ. Prior studies of the phase behavior for binary blends of semiflexible polymers indicate that the main influence of chain semiflexibility enters primarily through the difference $E_b^{(1)} - E_b^{(2)}$ in the "bending" energies for the two components.[13,25] Thus, we vary $E_b^{(1)} - E_b^{(2)}$ to determine if stiffness disparity can produce large negative A. The fitting procedure employs two adjustable parameters (ϵ and $E_b^{(1)} - E_b^{(2)}$). We find a wide range of parameter pairs that produce good agreement with experiment, and Figure 7 illustrates two examples. Reasonably good fits to experiment can be generated for ϵ in the range (at least) between $\epsilon = -0.0166$ K and $\epsilon = +0.000415$ K and for $E_b^{(1)} - E_b^{(2)} \approx 290$ K. These miniscule values of the microscopic exchange energy ϵ (on a per site basis) accord with our expectation that PP and hhPP are almost identical from an interaction energy standpoint. The greater steric interactions between the neighboring side groups in hhPP is likewise anticipated[13] to render hhPP stiffer than PP, in accord with our fit parameters that yield E_b(hhPP) > E_b(PP).

V. Discussion

Imposition of the high pressure, high molecular weight limit to the lattice cluster theory (LCT) expression for the noncombinatorial free energy produces a remarkably simple and compact equation that is useful for analyzing experimental data and for probing general physical trends. The limiting LCT free energy of mixing is used to derive a similarly simple expressions for the small angle neutron scattering effective interaction parameter χ, which emerges from the LCT in the form of $\chi = A + B/T$ for blends of fully flexible polymer chains, where the temperature independent portion A of χ (the

so-called "entropic χ" parameter) is a measure of monomer structural disparity between the blend components. While A and B correspond to entropic and enthalpic contributions, respectively, *in a thermodynamic sense*, the simple *microscopic* interpretation of A as purely "entropic" (i.e., as emerging in the limit of infinite temperature) loses its validity when the systems are treated as compressible or when the polymer chains are allowed to be semiflexible. The LCT contributions to the "enthalpic" portion B of χ (see eq 11) represent a rigorous extension to structured monomers of the heuristic surface fraction concept inherent in the Guggenheim approximation, originally derived[34] for systems of linear flexible polymer chains.

Several illustrative examples are chosen to describe the various molecular factors influencing the miscibilities of binary polyolefin blends. The incompressible limit implies that the computed excess thermodynamic properties depend on only a single interaction energy ϵ, which is readily determined by fitting the LCT eq 11 to experimental data for the temperature dependence of χ. The theory provides an excellent estimation for the "entropic" A portion of χ for blends of poly(isobutylene) with head-to-head poly(propylene). The incompressible limit LCT expressions in eq 11 explain the common occurrence of LCST phase diagrams in blends of poly(isobutylene) with other polyolefins as arising from a competition between the stabilizing influence of a negative exchange energy ϵ and the entropic destabilization from the structural disparity between the PIB and other polyolefin monomers. The theory also predicts a weak molecular weight dependence on the critical temperatures of these LCST systems in accord with observations.

On an even simpler level, the chemical similarity of polyolefins motivates the assumption that the exchange energy ϵ is generally rather small, whereupon the critical temperature is a linear function of the entropic structural parameter (the A part of χ). This correlation may be applied (with the extensions given elsewhere[38]) to random copolymer systems. Illustrations of this simple correlation are described here for blends with either LCST or UCST phase diagrams.

The purely flexible chain limit expressions in eq 11 display the (incompressible, high molecular weight, flexible chain limit) "entropic" part A of χ as always nonnegative, in sharp contrast to experimental observations of rather large negative A for numerous binary polyolefin blends. A large negative A is particularly perplexing because this A corresponds naively to an *extra* entropy beyond the Flory combinatorial entropy that generally represents an *overcounting* of chain configurations for flexible polymers. The explanation of this discrepancy emerges directly from the extension of the LCT to systems of semiflexible polymers. The semiflexible LCT describes the chain stiffness through the presence of Boltzmann factors containing conformational energy differences (cf., eq 15). These conformational energy Boltzmann factors enter into both the A and B portions of the LCT χ and thereby invalidate the interpretations of A and B as arising microscopically from "entropic" and "enthalpic" origins, respectively. A further scrambling of microscopic contributions to the thermodynamic entropic and enthalpic portions to χ emerges from considering the systems as compressible.[39] These features caution against the automatic microscopic modeling of A and B with purely packing and interaction effects, respectively. The latter is highlighted by our analysis of the SANS data for PP/DhhPP blends, which yields a rather miniscule exchange energy in accord with the energetic near chemical identity of these two polymer species. On the other hand, analyzing the same SANS data with conventional Flory−Huggins theory yields a PP/DhhPP exhchange energy comparable to that observed for highly immiscible systems.

The high molecular weight, high-pressure limit of the LCT may likewise be applied to blends of polymers other than polyolefins. For example, LCT computations for blends of polystyrene with poly(*n*-alkyl methacralates) accord with experimental observations[40] of large A parameters. While this incompressible limit of the LCT is immensely useful for studying the molecular factors affecting miscibilities and effective interactions in polymer blends, the description of real systems at ambient pressures and lower molecular weights requires the use of the compressible LCT.

Acknowledgment. This research is supported, in part, by Grant No. DAAG55-97-1-0162 from ARO.

Appendix: Relationship between Experimental and LCT SANS Interaction Parameters

As noted in section III, the LCT effective interaction parameter χ_{site} is defined for a binary incompressible blend as

$$\chi_{\text{site}} = \frac{1}{2}\left[\frac{1}{M_1\varphi} + \frac{1}{M_2(1-\varphi)} - \left.\frac{\partial^2\{F/N_1kT\}}{\partial\varphi^2}\right|_{V,T}\right] \quad \text{(A1)}$$

where M_1 and M_2 are the numbers of sites occupied by individual chains of species 1 and 2. On the other hand, the experimental SANS parameter χ_{exp} is usally determined from the zero angle scattering intensity $I(0)$ as

$$\chi_{\text{exp}} = \frac{1}{2}v_0\left[\frac{1}{N_1\varphi v_1} + \frac{1}{N_2(1-\varphi)v_2} - \frac{k_{\text{N}}}{I(0)}\right] \quad \text{(A2)}$$

where N_α and v_α denote the polymerization index and the molar monomer volume of species α, respectively, $v_0 = (v_1v_2)^{1/2}$ is the arbitrarily chosen normalization volume, and the scattering contrast factor $k_{\text{N}} = (b_1/v_1 - b_2/v_2)^2N_0$ is represented in terms of the monomer scattering lengths b_α with N_0 as Avogadro's number. In the incompressible blend limit, the LCT scattering intensity $I(0)$ becomes a function of only one scattering factor (e.g., $S_{11}(0)$)

$$I(0) = \text{S}_{11}(0)\left[\frac{b_1}{s_1} - \frac{b_2}{s_2}\right]^2\frac{1}{v_{\text{cell}}} \quad \text{(A3)}$$

where s_α indicates the number of lattice sites occupied by a single monomer of species α, v_{cell} designates the volume associated with a single lattice site, and $S_{11}(0)$ is a second derivative of the free energy

$$\frac{1}{S_{11}(0)} = \left.\frac{\partial^2\{F/N_1kT\}}{\partial\varphi^2}\right|_{\text{V,T}} \quad \text{(A4)}$$

Given the assumption of blend incompressibility, the volume $\bar{v}_{\text{cell}}$ of a mole of lattice sites is expressed as

$$\bar{v}_{\text{cell}} = N_0v_{\text{cell}} = \left(\frac{v_1v_2}{s_1s_2}\right)^{1/2} \quad \text{(A5)}$$

Substituting eqs A3−A5 into the definition A2 converts the latter to the form

$$\chi_{exp} = \frac{1}{2}\left[\frac{1}{N_1\varphi}\left(\frac{v_2}{v_1}\right)^{1/2} + \frac{1}{N_2(1-\varphi)}\left(\frac{v_1}{v_2}\right)^{1/2} - \frac{v_1 v_2[b_1/v_1 - b_2/v_2]^2}{(s_1 s_2)^{1/2}[b_1/s_1 - b_2/s_2]^2 S_{11}(0)}\right] \quad \text{(A6)}$$

Assuming perfect contrast ($b_2 = 0$) reduces eq (A6) to

$$\chi_{exp} = \frac{1}{2}\left[\frac{1}{N_1\varphi}\left(\frac{v_2}{v_1}\right)^{1/2} + \frac{1}{N_2(1-\varphi)}\left(\frac{v_1}{v_2}\right)^{1/2} - \frac{v_2}{v_1}\frac{s_1^{\,2}}{(s_1 s_2)^{1/2}}\frac{1}{S_{11}(0)}\right] \quad \text{(A7)}$$

Combining eqs A1, A2, A4, and A7 enables us to relate the LCT χ_{site} to the experimental χ_{exp} through

$$\chi_{exp} = \frac{1}{2}\left[\frac{1}{N_1\varphi}\left(\frac{v_2}{v_1}\right)^{1/2} + \frac{1}{N_2(1-\varphi)}\left(\frac{v_1}{v_2}\right)^{1/2} - \frac{v_2}{v_1}\frac{s_1^{\,2}}{(s_1 s_2)^{1/2}}\left(\frac{1}{M_1\varphi} + \frac{1}{M_2(1-\varphi)} - 2\chi_{site}\right)\right] \quad \text{(A8)}$$

After some simple algebra, eq A.8 becomes transformed into the more convenient form

$$\chi_{exp} = \frac{1}{2}\frac{v_2}{v_1}\left[\frac{1}{N_1\varphi}\left\{\left(\frac{v_1}{v_2}\right)^{1/2} - \left\{\frac{s_1}{s_2}\right\}^{1/2}\right\} + \frac{1}{N_2(1-\varphi)}\left\{\left(\frac{v_1}{v_2}\right)^{3/2} - \left\{\frac{s_1}{s_2}\right\}^{3/2}\right\} + 2\chi_{site}\frac{s_1^{\,2}}{(s_1 s_2)^{1/2}}\right] \quad \text{(A9)}$$

where use has been made of the relation

$$M_\alpha = N_\alpha s_\alpha, \quad \alpha = 1, 2 \quad \text{(A10)}$$

Choosing the ratio of monomer site occupancy indices s_1/s_1 to coincide with the ratio v_1/v_2 of monomer molecular volumes makes the first two terms in braces of eq A9 vanish identically, yielding the simple scaling between the customary experimental and the incompressible LCT interaction parameters as

$$\chi_{exp} = \chi_{site}\frac{v_2}{v_1}\frac{s_1^{\,2}}{(s_1 s_2)^{1/2}} = \chi_{site}(s_1 s_2)^{1/2} \quad \text{(A11)}$$

as quoted in eq 9.

Some experimental analyses include the temperature-dependent monomer specific volumes v_α in eq A2. To incorporate this variation with the incompressible limit LCT, eq A10 must be used instead.

References and Notes

(1) Flory, P. J. *J. Chem. Phys.* **1941**, *9*, 660; *Principles of Polymer Chemistry*; Cornell Press: Ithaca, NY, 1953.
(2) Janssen, S.; Schwahn, D.; Mortensen, K.; Springer, T. *Macromolecules* **1993**, *26*, 5589. Hammouda, B.; Bauer, B. J. *Macromolecules* **1995**, *28*, 4505.
(3) Freed, K. F.; Dudowicz, J. *Trends Polym. Sci.* **1995**, *3*, 248.
(4) Dudowicz, J.; Freed, K. F. *Macromolecules* **1991**, *24*, 5076.
(5) Nemirovsky, A. M.; Bawendi, M. G.; Freed, K. F. *J. Chem. Phys.* **1987**, *87*, 7272.
(6) (a) Freed, K. F.; Bawendi, M. G. *J. Phys. Chem.* **1989**, *93*, 2194. (b) Dudowicz, J.; Freed, K. F.; Madden, W. G. *Macromolecules* **1990**, *23*, 4803.
(7) Freed, K. F.; Pesci, A. I. *J. Chem. Phys.* **1987**, *87*, 7342.
(8) Dudowicz, J.; Freed, M. S.; Freed, K. F. *Macromolecules* **1991**, *24*, 5096. Dudowicz, J.; Freed, K. F. *Macromolecules* **1991**, 24, 5112. Freed, K. F.; Dudowicz, J. *Theor. Chim. Acta* **1992**, *82*, 357.
(9) Freed, K. F.; Dudowicz, J. *Macromolecules* **1996**, *29*, 625.
(10) Dudowicz, J.; Freed, K. F. *Macromolecules* **1996**, *29*, 7826.
(11) Dudowicz, J.; Freed, K. F. *Macromolecules* **1993**, *26*, 213.
(12) This behavior has subsequently been observed by: Russell, T. P.; Karis, T. E.; Gallot, Y.; Mayes, A. M. *Nature* **1994**, *368*, 729. Karis, T. E.; Russell, T. P.; Gallot, Y.; Mayes, A. M. *Macromolecules* **1995**, *28*, 1129.
(13) Freed, K. F.; Dudowicz, J.; Foreman, K. W. *J. Chem. Phys.* **1998**, *108*, 7881.
(14) Graessley, W. W.; Krishnamoorti, R.; Reichart, G. C.; Balsara, N. P.; Fetters, L. J.; Lohse, D. J. *Macromolecules* **1995**, *28*, 1260.
(15) Kumar, S. K. *Macromolecules* **1994**, *27*, 260. Kumar, S. K.; Veytsman, B. A.; Maranas, J. K.; Crist, B. *Phys. Rev. Lett.* **1997**, *79*, 2265.
(16) Joanny, J.-F.; Benoit, H. *Macromolecules* **1997**, *30*, 3704.
(17) Higgins, J.; Benoit, H. *Polymers and Neutron Scattering*; Clarendon Press: Oxford, England 1994; Taylor, J. K.; Debenedetti, P. G.; Graessley, W. W.; Kumar, S. K. *Macromolecules* **1996**, *29*, 764.
(18) We note in this regard that all atomistic off-lattice computations of polymer properties with Monte Carlo, molecular dynamics, and integral equation methods, of necessity, describe these systems as compressible, i.e., with densities lower than those corresponding to close packing.
(19) Tang, H.; Freed, K. F. *Macromolecules* **1991**, *24*, 958. Hammouda, B. *J. Non-Cryst. Solids* **1994**, *172−174*, 928; Bidkar, U. R.; Sanchez, I. C. *Macromolecules* **1995**, *28*, 3963.
(20) Dudowicz, J.; Freed, K. F., *Macromolecules* **1990**, *23*, 1519.
(21) Sanchez, I. C.; Lacomb, R. H. *Macromolecules* **1978**, *11*, 1145.
(22) Flory, P. J.; Orwoll, R. A.; Vrij, A. *J. Am. Chem. Soc.* **1964**, *86*, 3507.
(23) Dee, G. T.; Walsh, D. J. *Macromolecules* **1988**, *21*, 811, 815. Lipson, J. E. G.; Andrews, S. S. *J. Chem. Phys.* **1992**, *96*, 1426.
(24) Bates, F. S.; Fredrickson, G. H., *Macromolecules* **1994**, *27*, 1065. Fredrickson, G. H.; Liu, A. J.; Bates, F. S., *Macromolecules* **1994**, *27*, 2503.
(25) (a) Foreman, K. W.; Freed, K. F. *Macromolecules* **1997**, *30*, 7295. (b) Foreman, K. W.; Freed, K. F. *Adv. Chem. Phys.* **1998**, *103*, 335.
(26) Madden, W. G. *J. Chem. Phys.* **1990**, *92*, 2055.
(27) Nemirovsky, A. M.; Dudowicz, J.; Freed, K. F. *Phys. Rev.* A **1992**, *45*, 7111.
(28) We assume here that there no penta-or higher functional groups are present.
(29) (a) Freed, K. F.; Dudowicz, J. *Macromolecules* **1996**, *29*, 625. (b) Dudowicz, J.; Freed, K. F. *Macromolecules* **1997**, *30*, 5506.
(30) The simplifications arise when all subchains in the side groups have at least a pair of sequential bonds. See appendix in ref 27.
(31) From Table 3 of ref 6b, using the relation in the Appendix of ref 27.
(32) Sariban, A.; Binder, K. *J. Chem. Phys.* **1997**, *86*, 5859.
(33) Foreman, K. W.; Freed, K. F.; Ngola, I. M. *J. Chem. Phys.* **1997**, *107*, 4688.
(34) Guggenheim, E. A. *Proc. R. Soc. London, A* **1944**, *183*, 203, 213; *Mixtures*; Oxford University Press: Oxford, England 1952.
(35) Foreman, K. W.; Freed, K. F., *J. Chem. Phys.* **1995**, *102*, 4663.
(36) Krishnamoorti, R.; Graessley, W. W.; Fetters, L. J.; Garner, R. T.; Lohse, D. J. *Macromolecules* **1995**, *28*, 1252.
(37) Singh, C.; Schweizer, K. S. *Macromolecules* **1995**, *28*, 8692; *J. Chem. Phys.* **1995**, 103, 5814; **1997**, *30*, 1490.
(38) Dudowicz, J.; Freed, K. F. *Macromolecules*, submitted for publication.
(39) This point is evident from Table 2 of ref 29a and has also been noted by Schweizer, K. S.; Curro, J. C. *Adv. Polym. Sci.* **1994**, *116*, 319.
(40) Ruzette, A.-V.; Mayes, A. M.; Banerjee, P.; Russell, T. P.; Pollard, M.; Jerome, R. *Bull. Am. Phys. Soc.* **1998**, *43*, 450.

MA980702X